nature immunology

Transcription factor Foxo3 controls the magnitude of T cell immune responses by modulating the function of dendritic cells

Anne S Dejean[1], Daniel R Beisner[1,4], Irene L Ch'en[1], Yann M Kerdiles[1], Anna Babour[1], Karen C Arden[2], Diego H Castrillon[3,4], Ronald A DePinho[3] & Stephen M Hedrick[1]

Foxo transcription factors regulate cell cycle progression, cell survival and DNA-repair pathways. Here we demonstrate that deficiency in Foxo3 resulted in greater expansion of T cell populations after viral infection. This exaggerated expansion was not T cell intrinsic. Instead, it was caused by the enhanced capacity of Foxo3-deficient dendritic cells to sustain T cell viability by producing more interleukin 6. Stimulation of dendritic cells mediated by the coinhibitory molecule CTLA-4 induced nuclear localization of Foxo3, which in turn inhibited the production of interleukin 6 and tumor necrosis factor. Thus, Foxo3 acts to constrain the production of key inflammatory cytokines by dendritic cells and to control T cell survival.

Foxo transcription factors guide the cellular response to growth factors, nutrients and stress. This information is 'encoded' as post-translational modifications, referred to as the 'Foxo code', that govern Foxo intracellular localization, cofactor associations and transcriptional activity. The resulting program of gene expression regulates cell cycle arrest, repair, apoptosis and autophagy and many other aspects of cellular homeostasis[1]. In mammals, four Foxo members have been identified. Foxo1 (FKH1 and FKHR)[2], Foxo3 (FKHRL1; A000945)[3], and Foxo4 (AFX)[4] are widely expressed and similarly regulated, whereas expression of Foxo6 (ref. 5) is confined to specific structures of the brain and is subject to distinct regulatory mechanisms.

Insulin, insulin-like growth factor and other growth factors induce activation of phosphatidylinositol-3-OH kinase and the kinase Akt, which phosphorylate three Foxo amino acids[6]. These modifications result in the association of the Foxo protein with the adaptor protein 14-3-3 and the nuclear exclusion and eventual degradation of Foxo3 (refs. 7–9). This process can be actively opposed by stress-induced signals that activate the Jnk mitogen-activated protein kinase, which result in Foxo3 nuclear localization[10]. Foxo factor target specificity can be further refined by the SIRT1 deacetylase[11,12].

Given their involvement in coordinating cellular growth, proliferation and survival, we predicted that Foxo factors would be central to the highly dynamic, infection-mediated expansion and contraction of antigen-specific T cell populations. Indeed, Foxo activity is regulated by signaling by the T cell antigen receptor (TCR) and CD28, as well as by cytokines such as interleukin 2 (IL-2)[13], IL-3 (ref. 14) and IL-7 (refs. 15,16). These stimuli result in the phosphorylation of Foxo by Akt, the kinase Sgk or inhibitor of transcription factor NF-κB (IκB) kinase, and in Foxo3 nuclear exclusion[17]. Withdrawal of growth factor causes dephosphorylation of nuclear Foxo3, binding of Foxo3 to the promoters of the genes encoding the proapoptotic molecules Bim and Puma, induction of transcription of those genes, and T cell apoptosis[18]. In contrast, enforced expression of a constitutively nuclear form of Foxo3 in T cell lines causes cell cycle arrest[13]. Furthermore, Foxo3 is involved in the persistence of $CD4^+$ central memory T cells in mice and humans[19].

Published studies have shown spontaneous T cell activation, lymphoproliferative disease and organ infiltration in '*Foxo3*^{Trap}' mice, which have a mutated *Foxo3* allele generated by gene-trap technology[20]. Such studies indicate an important function for Foxo3 in immune regulation, although the underlying molecular mechanisms are not understood. In addition, Foxo3 regulates superoxide dismutase in dendritic cells (DCs); this signaling pathway may affect the suppressive or stimulating characteristics of plasmacytoid DCs[21,22].

In this study, we sought to determine whether Foxo3 is involved in the quiescence of cells of the immune system and the dynamics of T cell population expansion and contraction. We found that in response to LCMV infection, Foxo3 deficiency caused superabundant expansion of antigen-specific T cell populations. However, contrary to our expectations, this phenotype was not intrinsic to T cells but instead arose from altered stimulatory properties of Foxo3-deficient DCs. Foxo3 deficiency resulted in a DC-specific higher production of

[1]Molecular Biology Section, Division of Biological Sciences, and Department of Cellular and Molecular Medicine, University of California, San Diego, San Diego, California, USA. [2]Ludwig Institute for Cancer Research, University of California, San Diego School of Medicine, La Jolla, California, USA. [3]Center for Applied Cancer Science, Belfer Institute for Innovative Cancer Science, Departments of Adult Oncology, Medicine and Genetics, Dana-Farber Cancer Institute, Harvard Medical School, Boston, Massachusetts, USA. [4]Present addresses: Genetics Institute of the Novartis Foundation, San Diego, California, USA (D.R.B.) and Department of Pathology, University of Texas, Southwestern Medical Center at Dallas, Dallas, Texas, USA (D.H.C.). Correspondence should be addressed to S.M.H. (shedrick@ucsd.edu).

Received 22 September 2008; accepted 19 March 2009; published online 12 April 2009; doi:10.1038/ni.1729

Table 1 Leukocyte subsets

Spleen	B6 *Foxo3*$^{+/+}$	B6 *Foxo3*^{Kca}	FVB *Foxo3*$^{+/+}$	FVB *Foxo3*$^{-/-}$
CD4$^+$	15.0 ± 2.0	17.3 ± 1.6	29.3 ± 5.1	31.0 ± 5.9
CD8$^+$	13.4 ± 3.5	9.7 ± 1.3	13.0 ± 2.2	14.9 ± 1.9
B220$^+$	46.9 ± 6.7	51.7 ± 9.2	58.2 ± 9.7	56.3 ± 12.1
Gr-1^{hi}CD11b^{hi}	1.4 ± 0.2	6.0 ± 1.1*	2.0 ± 0.2	5.4 ± 0.3*
Lymph node				
CD4$^+$	10.3 ± 1.4	9.4 ± 1.2	11.0 ± 2.5	12.8 ± 2.4
CD8$^+$	7.9 ± 1.0	7.3 ± 0.7	5.5 ± 1.2	7.0 ± 1.4
B220$^+$	13.8 ± 1.4	12.4 ± 1.1	4.0 ± 1.2	3.6 ± 0.7

Results are presented as the number of cells × 10^6 (± s.e.m.). *, $P < 0.001$, wild-type versus *Foxo3*-deficient mice (two-sample *t*-test assuming equal variances). Data are representative of two experiments with five to six mice per group.

IL-6. Nuclear localization of Foxo3 induced by signals initiated by cytotoxic T lymphocyte–associated antigen 4 (CTLA-4; A000706) suppressed Toll-like receptor–induced production of IL-6. Our results collectively emphasize the importance of Foxo3 in restraining the production of inflammatory cytokines by DCs and T cell viability.

RESULTS

No spontaneous activation of Foxo3-deficient T cells

To examine the function of Foxo3 in the immune system, we used two independently derived *Foxo3*-null strains distinct from the *Foxo3*^{Trap} mutant[20]. One strain, called '*Foxo3*^{Kca}' here, was backcrossed to the C57BL/6 strain, whereas mice of the other strain, called '*Foxo3*$^{-/-}$' here, were maintained as congenic FVB mice. Although we detected strain-specific differences, deletion of *Foxo3* had no effect on the proportion of T cells or B cells in the spleens and lymph nodes of 6- to 10-week-old mice (**Table 1**). However, we noted a greater proportion of Gr-1^{hi}CD11b^{hi} cells, which include granulocytes and macrophages, in the spleens of both Foxo3-deficient strains. We detected neither lymphocytic organ infiltration nor lymphadenopathy[23] (data not shown) in 6- to 10-week-old Foxo3-deficient mice. However 3- to 6-month-old Foxo3-deficient mice had enlargement of the spleen and more erythrocyte progenitors (Ter119$^+$; data not shown). That observation probably relates to the shorter erythrocyte lifespan and lower rate of erythrocyte maturation in Foxo3-deficient mice reported before[24]. Next we measured the expression of CD69, CD44 and CD62L (L-selectin) on T cells from Foxo3-deficient mice and their wild-type littermates. Although we again detected differences between the C57BL/6 and FVB strains, inactivation of *Foxo3* had no effect on the proportion of activated (CD69^{hi}) or memory-effector (CD44^{hi}CD62L^{lo}) T cells (**Fig. 1a**).

Published studies have shown constitutive activation of the NF-κB pathway in *Foxo3*^{Trap} mice, as reflected by the absence of IκB[20]. However, T cells purified from *Foxo3*^{Kca} and *Foxo3*$^{-/-}$ mice showed no change in the expression of IκBα, IκBβ or IκBε protein relative to that of wild-type T cells (**Supplementary Fig. 1** online). To measure the effect of Foxo3 deficiency on T cell proliferation, we labeled purified lymph node T cells with the cytosolic dye CFSE and then cultured the cells with plate-bound antibody to CD3 (anti-CD3) with or without anti-CD28. Neither the number of cell divisions nor the accumulation of cells in each division was altered by Foxo3 deficiency (**Fig. 1b**). Also, freshly explanted *Foxo3*^{Kca} and wild-type CD4$^+$ and CD8$^+$ T cells produced similar amounts of cytokines (**Fig. 1c**). As FasL (CD95L), the ligand for the cell surface receptor Fas, is a known target of Foxo3, we also analyzed FasL expression on unstimulated and antibody-stimulated T cells from wild-type and *Foxo3*^{Kca} mice; however we found no differences related to Foxo3 status (data not shown). These results suggest that loss of Foxo3 alone is not sufficient to elicit manifestations of T cell activation and spontaneous autoimmunity.

Foxo3^{Kca} mice show enhanced T cell accumulation

As Foxo3 is involved in cell cycle progression and apoptosis[25], we sought to investigate its function in the dynamics of T cell population expansion and contraction in response to viral infection. Historically, the C57BL/6 strain has been used to study the progression of viral responses, and as the two mutant strains homozygous for Foxo3 deficiency had identical profiles here and in published results[23,26], our further efforts at characterization focused on the C57BL/6 *Foxo3*^{Kca} mice. We infected *Foxo3*^{Kca} mice and their wild-type littermates with

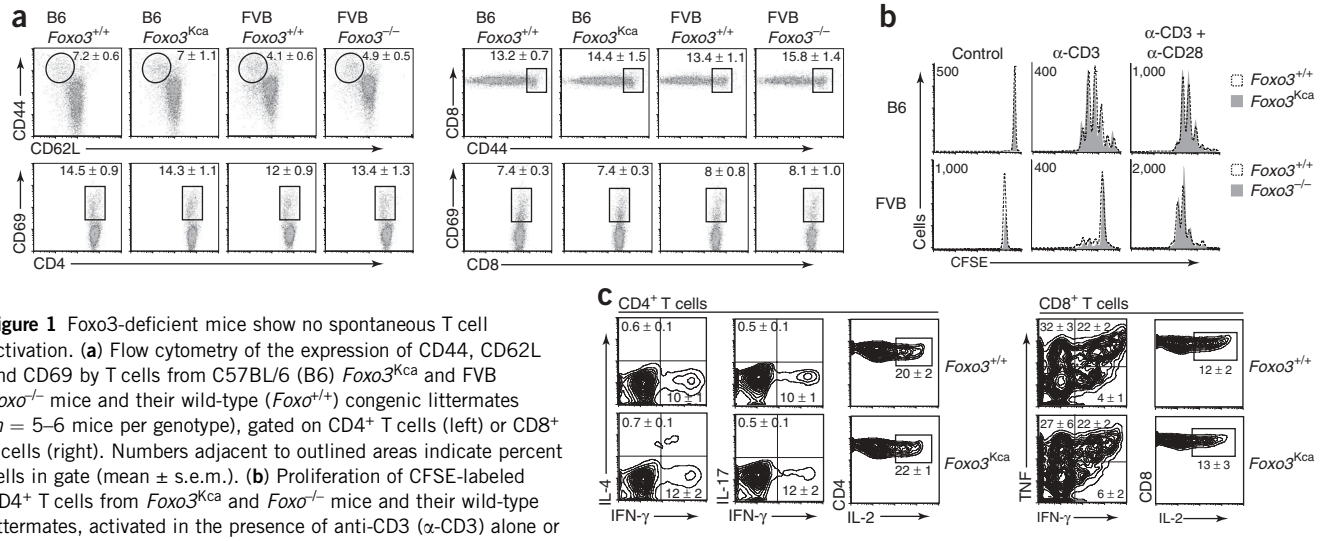

Figure 1 Foxo3-deficient mice show no spontaneous T cell activation. (**a**) Flow cytometry of the expression of CD44, CD62L and CD69 by T cells from C57BL/6 (B6) *Foxo3*^{Kca} and FVB *Foxo*$^{-/-}$ mice and their wild-type (*Foxo*$^{+/+}$) congenic littermates ($n = 5$–6 mice per genotype), gated on CD4$^+$ T cells (left) or CD8$^+$ T cells (right). Numbers adjacent to outlined areas indicate percent cells in gate (mean ± s.e.m.). (**b**) Proliferation of CFSE-labeled CD4$^+$ T cells from *Foxo3*^{Kca} and *Foxo*$^{-/-}$ mice and their wild-type littermates, activated in the presence of anti-CD3 (α-CD3) alone or with anti-CD28 (α-CD28) and assessed by CFSE dilution after 72 h of stimulation. Numbers in plots indicate number of accumulated CFSE$^+$ cells. (**c**) Cytokine secretion by splenocytes from *Foxo3*^{Kca} mice and their wild-type littermates ($n = 6$ mice per group), activated for 3 h in the presence of phorbol 12-myristate 13-acetate and ionomycin and analyzed by intracellular staining with gating on CD4$^+$ T cells (left) or CD8$^+$ T cells (right). Numbers in quadrants and adjacent to outlined areas indicate percent cells in each (mean ± s.e.m.). Similar results were obtained with lymph node T cells. Data are from five separate experiments (**a**) or are representative of three independent experiments (**b**,**c**).

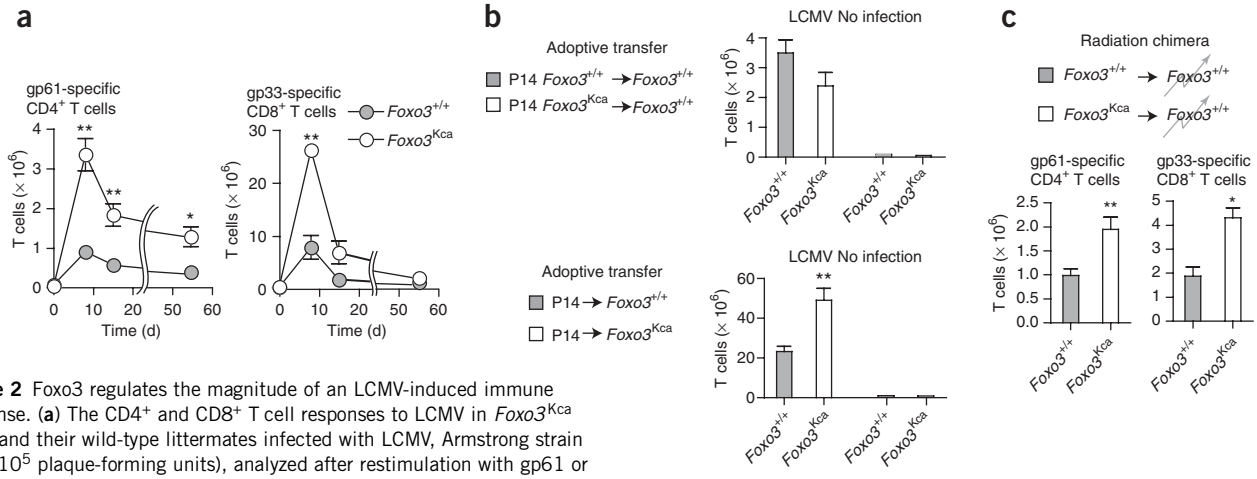

Figure 2 Foxo3 regulates the magnitude of an LCMV-induced immune response. (**a**) The CD4$^+$ and CD8$^+$ T cell responses to LCMV in *Foxo3*^{Kca} mice and their wild-type littermates infected with LCMV, Armstrong strain (2×10^5 plaque-forming units), analyzed after restimulation with gp61 or gp33 peptide, respectively, by intracellular staining for IFN-γ. (**b**) P14 T cells in recipient mice given CD45.2 congenic wild-type or *Foxo3*^{Kca} P14 T cells (transferred into (→) CD45.1 wild-type mice; top) and CD45.1 congenic wild-type P14 T cells (transferred into CD45.2 wild-type or CD45.2 *Foxo3*^{Kca} mice; bottom) and then left uninfected (right) or infected with LCMV (left) and assessed with a congenic marker 8 d later. (**c**) Virus-specific T cells in lethally irradiated (gray 'lightning bolt' around) CD45.1 wild-type mice reconstituted with CD45.2 congenic wild-type or *Foxo3*^{Kca} bone marrow and then infected with LCMV 8 weeks later, assessed by specific peptide restimulation and intracellular IFN-γ staining. *, $P < 0.01$, and **, $P < 0.005$ (unpaired two-tailed Student's *t*-test). Data are representative of four (**a**) or two (**b**,**c**) independent experiments with at least three mice per group (error bars, s.e.m.).

lymphocytic choriomeningitis virus (LCMV) and assessed LCMV-responsive T cell populations at various times after infection. Whereas the *Foxo3* genotype had no effect on the kinetics of T cell population expansion, *Foxo3*^{Kca} mice developed a threefold greater accumulation of LCMV-specific T cells than did their wild-type littermates (**Fig. 2**). Measurement of virus in the liver at day 8 after infection showed complete viral clearance in both strains (data not shown).

The lack of an effect of Foxo3 deficiency on T cells stimulated in culture prompted us to test whether the enhanced T cell accumulation during an LCMV response was T cell intrinsic. We transferred T cells from LCMV-specific TCR-transgenic P14 *Foxo3*^{Kca} or P14 wild-type mice into wild-type C57BL/6 mice and measured the accumulation of P14 T cells after infection of the recipient mice with LCMV. We detected no significant difference in the accumulation of *Foxo3*^{Kca} and wild-type P14 T cells (**Fig. 2b**). To further examine this issue, we transferred wild-type P14 T cells into either wild-type or *Foxo3*^{Kca} mice and infected recipients with LCMV. P14 T cells transferred into *Foxo3*^{Kca} mice accumulated in greater numbers than did P14 T cells transferred into wild-type hosts (**Fig. 2b**). We reproduced that result with the transfer of ovalbumin (OVA)-specific OT-I T cells into wild-type and *Foxo3*^{Kca} hosts that we subsequently infected with OVA-expressing vesicular stomatitis virus (**Supplementary Fig. 2** online).

To further investigate the cellular cause of the enhanced T cell population expansion, we reconstituted irradiated wild-type mice with bone marrow from wild-type or *Foxo3*^{Kca} mice. After 8 weeks, we infected the recipient mice with LCMV and analyzed expansion of the LCMV-specific T cell population. Excessive T cell accumulation was apparent in recipients of *Foxo3*^{Kca} bone marrow (**Fig. 2c**), which indicated involvement of a bone marrow–derived cell type in this phenotype. Thus, a non–T cell bone marrow–derived cell type was responsible for the enhanced T cell proliferation and/or survival in Foxo3-deficient mice.

Stimulatory capacity of DCs from *Foxo3*^{Kca} mice

The efficiency of antigen presentation can affect the magnitude of a T cell response to viral infection[27]. Therefore, we assessed whether Foxo3 regulates the number, phenotype and/or function of antigen-presenting DCs. Naive *Foxo3*^{Kca} mice had significantly more DCs than did their wild-type littermates (**Fig. 3a**), and there was a slightly greater proportion of DCs with high expression of the costimulatory molecules B7-1 (CD80) and B7-2 (CD86). We found no difference in the expression of major histocompatibility complex (MHC) class I, MHC class II or CD40 on DCs from these mice (**Fig. 3b**), which suggested that a small number of Foxo3-deficient DCs had a more mature phenotype.

Analysis of various DC subsets showed that Foxo3-deficient mice had more CD11c$^+$CD11b$^+$CD8$^-$, CD11c$^+$CD11b$^-$CD8$^+$ and CD11c$^+$B220$^+$ DCs (**Fig. 3c**). All subsets showed a moderate shift toward high expression of B7-1 and B7-2 (**Fig. 3d**), although the biological importance of this shift is unclear. To further characterize the activation status of DCs from naive mice, we cultured splenic DCs overnight and then measured secreted cytokines. *Foxo3*^{Kca} DCs produced more IL-6, tumor necrosis factor (TNF) and chemokine CCL2 (MCP-1) than did wild-type DCs (**Fig. 3e**). Interferon-γ (IFN-γ), IL-10 and IL-12 were undetectable (data not shown).

To determine whether DCs from *Foxo3*^{Kca} mice had enhanced antigen presentation, we infected mice with LCMV and analyzed DCs 3 d after infection, when virus is still present and T cell populations are expanding exponentially[28]. Compared with wild-type DCs, *Foxo3*^{Kca} DCs had slightly higher expression of B7-1, B7-2 and MHC class II (**Fig. 4a**) and more effectively stimulated the accumulation of P14 T cells, as measured by CFSE dilution and staining with annexin V and 7-amino-actinomycin D (7-AAD; **Fig. 4b**). This enhanced stimulatory capacity was not due to a difference in antigen processing, as differences between cultures with *Foxo3*^{Kca} and wild-type DCs remained even after DCs were pulsed with LCMV glycoprotein 33 (gp33) peptide (**Fig. 4b**).

To rule out the possibility that Foxo3-deficient DCs from LCMV-infected mice can cause proliferation of bystander T cells independently of the presence of antigen, we also cultured DCs from LCMV-infected mice with OT-I T cells with or without OVA peptide (amino acids 257–264; OVA (257–264)). In the absence of OVA (257–264), there was no detectable division of OT-I T cells (**Fig. 4b**), which ruled out the possibility of bystander effects. Finally,

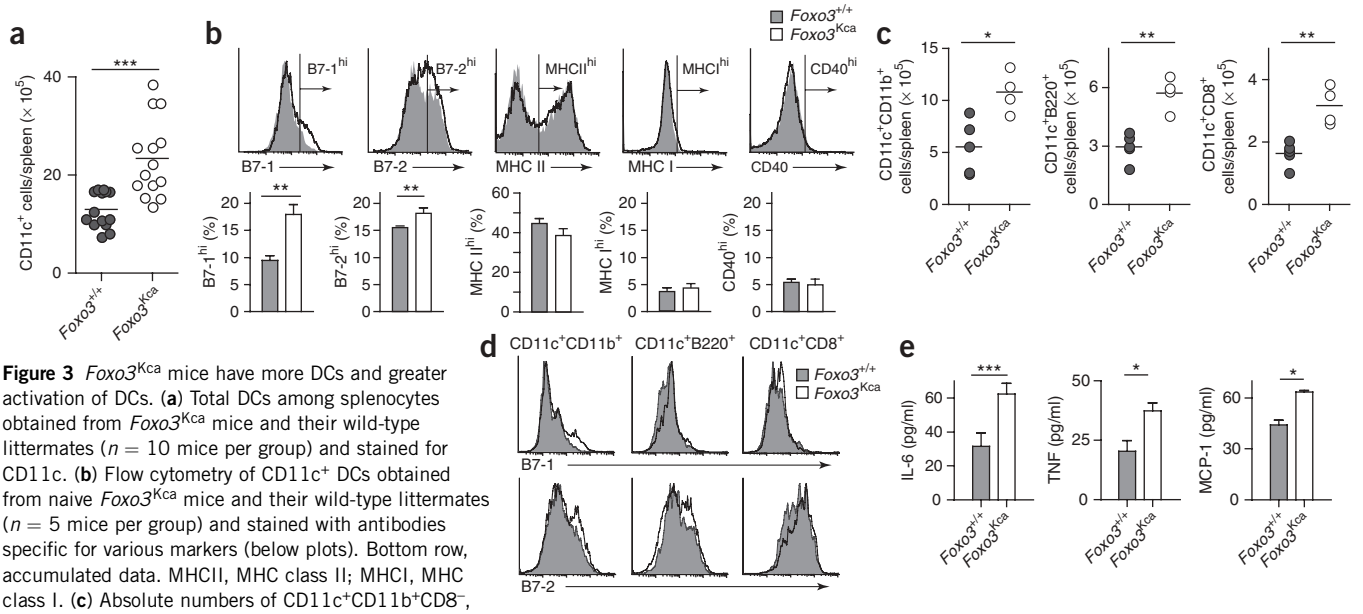

Figure 3 *Foxo3*^{Kca} mice have more DCs and greater activation of DCs. (**a**) Total DCs among splenocytes obtained from *Foxo3*^{Kca} mice and their wild-type littermates ($n = 10$ mice per group) and stained for CD11c. (**b**) Flow cytometry of CD11c$^+$ DCs obtained from naive *Foxo3*^{Kca} mice and their wild-type littermates ($n = 5$ mice per group) and stained with antibodies specific for various markers (below plots). Bottom row, accumulated data. MHCII, MHC class II; MHCI, MHC class I. (**c**) Absolute numbers of CD11c$^+$CD11b$^+$CD8$^-$, CD11c$^+$CD11b$^-$CD8$^+$ and CD11c$^+$B220$^+$ DCs in spleens of *Foxo3*^{Kca} mice and their wild-type littermates ($n = 5$ mice per group). (**d**) Flow cytometry of the expression of B7-1 and B7-2 on DC subsets (above plots) from *Foxo3*^{Kca} mice and their wild-type littermates. (**e**) Cytokine bead array analysis of the concentration of IL-6, TNF and CCL2 (MCP-1) in supernatants of splenic DCs (CD11c$^+$) purified from wild-type or *Foxo3*^{Kca} mice and cultured for 24 h (4×10^5 cells). In **a**,**c**, each symbol represents an individual mouse; small horizontal lines indicate the mean. *, $P < 0.01$; **, $P < 0.005$; and ***, $P < 0.001$ (unpaired two-tailed Student's *t*-test). Data are representative of three independent experiments (**a**,**b**) or two independent experiments with at least three mice per group (**c**–**e**; error bars (**b**,**e**), s.e.m.).

we measured the capacity of DCs from uninfected mice to stimulate P14 T cells in the presence of gp33 peptide. We noted slightly greater accumulation and viability of T cells from cultures containing *Foxo3*^{Kca} DCs than from those containing wild-type DCs (**Fig. 4c**).

To determine if the enhanced function of Foxo3-deficient DCs was cell autonomous, we generated DCs *in vitro*. For this, we cultured bone marrow cells for 8 d with granulocyte-macrophage colony-stimulating factor. The number and proportion of the resulting CD11c$^+$ cells (called 'BMDCs' here) were unaffected by Foxo3 status, and none of the BMDCs had higher expression of B7-1, B7-2, CD40, MHC class I or MHC class II (**Supplementary Fig. 3a** online). Consistent with published reports of cells stimulated with granulocyte-macrophage colony-stimulating factor, wild-type BMDCs had a uniformly cytoplasmic Foxo3 localization[29] (**Supplementary Fig. 3b**). Next we used BMDCs to stimulate OT-II and P14 T cells at various ratios of T cells to DCs. *Foxo3*^{Kca} BMDCs induced accumulation of OT-II and P14 T cells more effectively than did wild-type BMDCs (**Fig. 5a**). Moreover, the Foxo3-deficient BMDCs also more effectively sustained T cell viability, regardless of cell division (**Fig. 5b**,**c**). To determine whether the differences in viability correlated with changes in Bcl-2 family members, we analyzed expression of the prosurvival factors Bcl-2 and Bcl-x$_L$. Total and naive CD44^{lo} T cells had higher expression of both when stimulated with Foxo3-deficient BMDCs (**Fig. 5d**).

To assess the capacity of BMDCs to enhance T cell survival *in vivo*, we transferred CFSE-labeled OT-II T cells into naive CD45.1 congenic hosts. Then, 1 d later, we transferred wild-type or Foxo3-deficient BMDCs, with or without preloaded OVA peptide (amino acids 323–339; OVA(323–339), into the footpads of these mice. After 2 additional days, *Foxo3*^{Kca} BMDCs induced a greater accumulation of OT-II T cells in the draining lymph nodes but a similar number of OT-II T cell divisions, compared with wild-type DCs (**Fig. 5e**). Notably, *Foxo3*^{Kca} DCs facilitated greater OT-II T cell survival, even in the absence of OVA(323–339). These data collectively establish that Foxo3-deficient DCs produce greater antigen-induced T cell population expansion by enhancing survival.

Enhanced IL-6 secretion by *Foxo3*-deficient DCs

To determine if the enhanced T cell survival induced by Foxo3-deficient DCs was due to altered cytokine secretion, we infected wild-type and *Foxo3*^{Kca} mice with LCMV and measured cytokine concentrations in blood plasma at various times after infection. The concentrations of IL-12, IL-17, CCL2 (MCP-1), IL-1β, IL-5, IL-10 were similar in wild-type and *Foxo3*^{Kca} mice (**Supplementary Fig. 4a** online), but the concentrations of IL-6 and TNF were higher in Foxo3-deficient mice (**Fig. 6a** and **Supplementary Fig. 4a**). To determine if DCs were the source of this abundant IL-6 and TNF, we collected splenic DCs from mice on day 3 after infection and cultured the cells for 24 h. Supernatants of *Foxo3*^{Kca} DC cultures had significantly higher concentrations of IL-6, TNF, CCL2 (MCP-1) and IFN-γ (**Fig. 6b** and **Supplementary Fig. 4b**), whereas we detected no difference in the concentration of IL-10 or IL-12. We also found higher expression of IL-6 mRNA in *Foxo3*^{Kca} DCs (**Fig. 6b**).

To determine whether cells other than DCs could be responsible for the greater IL-6 production, we collected T cells, B cells and macrophages from mice 3 d after LCMV infection and cultured the cells for 24 h. Neither T cells nor B cells had detectable production of IL-6 (data not shown). Macrophages did produce IL-6, although there was no difference related to *Foxo3* status (data not shown). However, given the finding of more macrophages in Foxo3-deficient mice, these cells may have contributed to the excess IL-6 production *in vivo*.

We next determined whether BMDCs also produced excess IL-6 in the absence of Foxo3. We detected significantly more IL-6 in cultures containing OT-II CD4$^+$ T cells or OT-I CD8$^+$ T cells and *Foxo3*^{Kca} BMDCs than in those containing T cells and wild-type DCs (**Fig. 6c**). Confirming the DC-specific nature of this abundant IL-6, RT-PCR

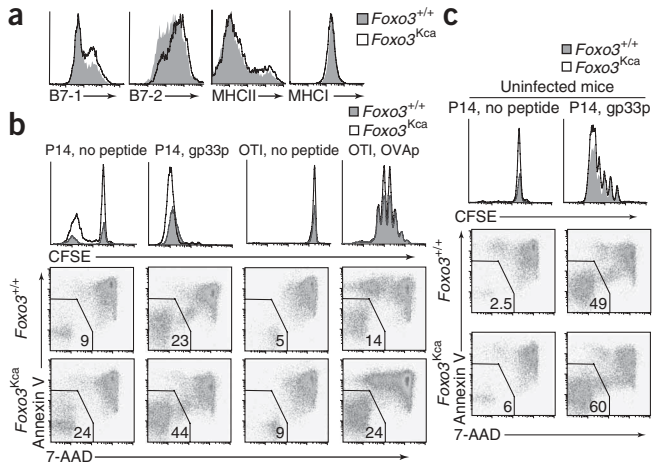

Figure 4 Greater immunogenicity of LCMV-infected *Foxo3*-deficient DCs. (**a**) Flow cytometry of the expression of activation markers on wild-type and *Foxo3*^{Kca} DCs on day 3 after LCMV infection. (**b**) Proliferation and viability of CFSE-labeled wild-type P14 CD8$^+$ T cells stimulated by DCs isolated from LCMV-infected *Foxo3*^{Kca} mice or their wild-type littermates (day 3) in the presence or absence of gp33 peptide (gp33p; left), or of CFSE-labeled wild-type OT-I CD8$^+$ T cells stimulated in the presence or absence of OVA (323–339) (OVAp; bystander proliferation; right), assessed by CFSE dilution (proliferation; top row) or staining with annexin V and 7-AAD after 3 d of culture (viability; middle and bottom rows). Numbers in dot plots indicate percent live CD8$^+$ T cells. (**c**) Proliferation and viability of T cells from P14 mice stimulated by DCs purified from the spleens of uninfected mice, cultured and analyzed as described in **b**. Data are representative of two independent experiments with at least three mice per group (**a**,**c**) or three independent experiments (**b**).

showed that *Foxo3*^{Kca} BMDCs had twofold more IL-6 mRNA than did wild-type BMDCs; IL-6 mRNA was at least tenfold greater in BMDCs than in CD4$^+$ T cells, and IL-6 mRNA was undetectable in CD8$^+$ T cells (**Fig. 6d**).

In combination with transforming growth factor-β, IL-6 induces the differentiation of IL-17-producing T cells[30]. Given the results presented above, we analyzed the balance between IL-17-producing T cells and Foxp3$^+$ regulatory T cells in Foxo3-deficient mice. The proportion of Foxp3$^+$ and IL-17$^+$ CD4$^+$ T cells in naive LCMV-infected *Foxo3*^{Kca} mice was similar to that of their wild-type littermates (**Supplementary Fig. 5** online). We did not detect IL-17-producing cells in the CD8$^+$ lineage (data not shown).

To evaluate whether the excess IL-6 produced by Foxo3-deficient DCs was required for their ability to induce enhanced T cell survival, we cultured OT-II and P14 T cells with BMDCs in the presence of an IL-6-specific blocking antibody or an immunoglobulin G1 (IgG1) isotype-matched control antibody. IL-6 blockade diminished the expansion of T cell populations cultured with *Foxo3*^{Kca} BMDCs to an amount resembling that of T cells cultured with wild-type DCs (**Fig. 6e**). Counting of dead cells stained with 7-AAD demonstrated

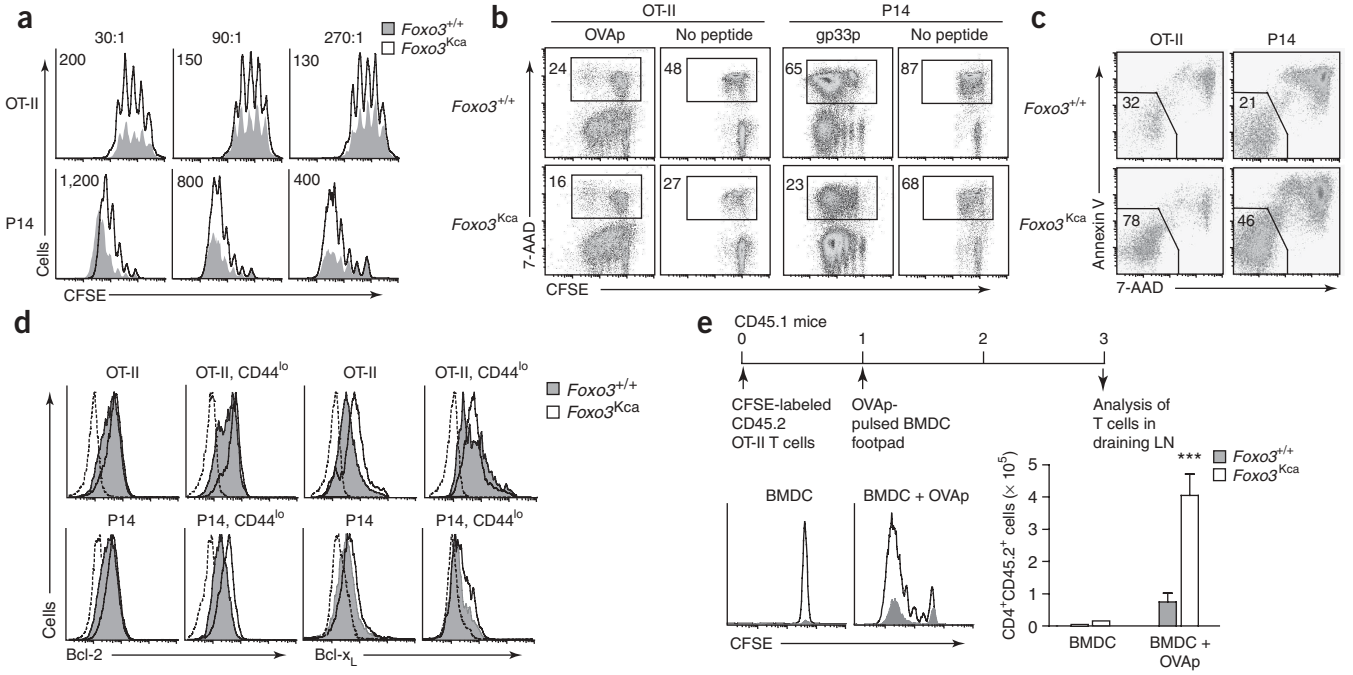

Figure 5 Enhanced T cell responses induced by *Foxo3*^{Kca} BMDCs. (**a**) CFSE-dilution analysis of the accumulation of wild-type OT-II CD4$^+$ T cells or wild-type P14 CD8$^+$ T cells stimulated for 3 d at various ratios (above plots) with wild-type or *Foxo3*^{Kca} BMDCs in the presence of OVA(323–339) (for OT-II T cells) or gp33 peptide (for P14 T cells). Numbers in plots indicate number of accumulated CSFE$^+$ cells. (**b**) Death of OT-II CD4$^+$ T cells or P14 CD8$^+$ T cells (1×10^5) cultured with wild-type or *Foxo3*^{Kca} BMDCs (3.3×10^2) in the presence or absence of the appropriate peptide, assessed by 7-AAD staining. Numbers adjacent to outlined areas indicate percent 7-AAD$^+$ T cells. (**c**) Viability of OT-II CD4$^+$ T cells or P14 CD8$^+$ T cells cultured for 3 d with BMDCs in the presence or absence of the appropriate peptide and stained with annexin V and 7-AAD. Numbers in outlined areas indicate percent viable CD4$^+$ or CD8$^+$ T cells. (**d**) Flow cytometry of the expression of Bcl-2 and Bcl-x_L in total T cells or gated CD44^{lo} T cells among OT-II or P14 T cells cultured as described in **b**. Dashed lines, isotype-matched control antibody. (**e**) Proliferation (left) and number (right) of CD4$^+$ T cells purified from wild-type CD45.2 OT-II mice, labeled with CFSE and injected intravenously into CD45.1 recipient mice, followed by subcutaneous injection of unpulsed or OVA(323–339)-pulsed (+ OVAp) BMDCs from *Foxo3*^{Kca} mice or their wild-type littermates ($n = 4$ mice per group) into the footpads of the same recipient mice and analysis 3 d later. Left, CFSE-dilution analysis; right, CD45.1 cells in draining lymph nodes (LN). Data are representative of at least six independent experiments (**a**,**b**) or two (**c**,**d**) or three (**e**) independent experiments (error bars (**e**), s.e.m.).

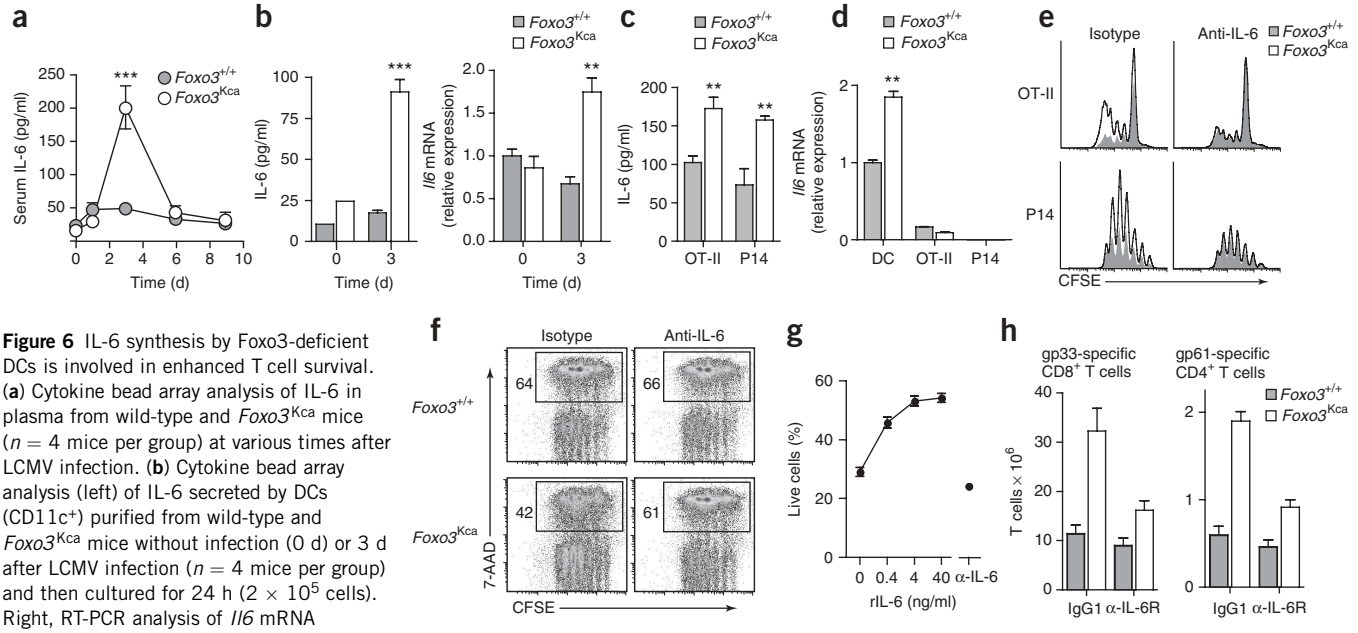

Figure 6 IL-6 synthesis by Foxo3-deficient DCs is involved in enhanced T cell survival. (**a**) Cytokine bead array analysis of IL-6 in plasma from wild-type and *Foxo3*^{Kca} mice ($n = 4$ mice per group) at various times after LCMV infection. (**b**) Cytokine bead array analysis (left) of IL-6 secreted by DCs (CD11c$^+$) purified from wild-type and *Foxo3*^{Kca} mice without infection (0 d) or 3 d after LCMV infection ($n = 4$ mice per group) and then cultured for 24 h (2×10^5 cells). Right, RT-PCR analysis of *Il6* mRNA expression, presented relative to the expression in uninfected wild-type cells, set as 1. (**c**) Enzyme-linked immunosorbent assay of IL-6 in supernatants of wild-type OT-II or P14 T cells cultured for 3 d in the presence of wild-type or *Foxo3*^{Kca} BMDCs loaded with OVA(323–339) or gp33 peptide. (**d**) RT-PCR analysis of *Il6* mRNA in BMDCs (DC), OT-II T cells and P14 T cells purified after 2 d of culture as described in **c**, presented relative to *Gapdh* mRNA (encoding glyceraldehyde phosphate dehydrogenase). (**e**,**f**) Accumulation (**e**) and death (**f**) of wild-type OT-II or P14 T cells activated by BMDCs generated from wild-type or *Foxo3*^{Kca} mice pulsed with OVA(323–339) (for OT-II CD4$^+$ T cells) or gp33 peptide (for P14 CD8$^+$ T cells), in the presence of an IgG1 isotype-matched control antibody or IL6-specific blocking antibody (10 μg/ml), assessed after 3 d of culture by CFSE dilution (accumulation) or 7-AAD staining (death). Numbers adjacent to outlined areas (**f**) indicate percent dead 7-AAD$^+$CFSE$^+$ cells. (**g**) Death of P14 T cells stimulated by wild-type BMDCs in the presence of increasing amounts of recombinant IL-6 (rIL-6) or IL-6-specific blocking antibody (α-IL-6), assessed after 3 d of culture by 7-AAD staining. (**h**) LCMV-specific T cell responses of *Foxo3*^{Kca} mice and their wild-type littermates ($n = 4$ mice per group) treated on days –1 and +4 with 100 μg of antibody to IL-6 receptor α-chain (α-IL-6R) or isotype-matched control antibody (IgG1) and infected on day 0 with LCMV, Armstrong strain, and then analyzed on day +8 by counting of P14 CD8$^+$ T cells and OT-II CD4$^+$ T cells producing IFN-γ after restimulation with OVA(323–339) (for OT-II CD4$^+$ T cells) or gp33 peptide (for P14 CD8$^+$ T cells). Data are representative of three (**a**–**f**) or two (**g**,**h**) independent experiments (error bars (**a**–**d**,**g**,**h**), s.e.m.).

that this reversion was due to lower T cell survival (**Fig. 6f**). In addition, we determined whether exogenous IL-6 was sufficient to enhance the survival of T cells cultured with wild-type BMDCs. Indeed, we noted a direct correlation between the amount of IL-6 added and the proportion of live T cells in each culture[31] (**Fig. 6g**).

To directly ascertain if IL-6 was responsible for the greater expansion of T cell populations in response to LCMV, we treated mice on days –1 and +4 (relative to LCMV infection at day 0) with 100 μg of blocking antibody to IL-6 receptor α-chain. Blockade of this receptor resulted in LCMV-specific T cell responses of substantially smaller magnitude in *Foxo3*-deficient mice but did not affect the number of LCMV-specific T cells in wild-type mice (**Fig. 6h**). These experiments collectively suggest that wild-type DCs are restrained from abundant IL-6 production by Foxo3 and thus that the factors that affect the localization and transcriptional activity of Foxo3 will influence the magnitude of a T cell–mediated immune response.

Foxo3 acts 'downstream' of CTLA-4-induced signals

Stimulation of B7 receptors by CTLA-4 promotes nuclear localization of Foxo3 and activation of DCs[32]. As cell surface CTLA-4 expression is induced on activated T cells, we analyzed whether signaling through the B7 receptor inhibits IL-6 production in a Foxo3-dependent way. We stimulated splenic DCs with loxoribine, a Toll-like receptor 7 agonist, in the presence of varying amounts of a fusion of CTLA-4 and immunoglobulin (CTLA-4–Ig). The production of IL-6 and TNF stimulated by loxoribine was strongly inhibited by CTLA-4–Ig in wild-type DCs but not in Foxo3-deficient DCs (**Fig. 7a**). Although treatment with CTLA-4–Ig resulted in a slightly greater proportion of dead cells, its toxic effects were equivalent in wild-type and *Foxo3*^{Kca} splenic DCs showed the same toxicity (**Fig. 7a**).

To confirm the involvement of Foxo3 in the inhibition of cytokine production induced by CTLA-4–Ig, we analyzed the intracellular localization of Foxo3 after stimulation with loxoribine or CTLA-4–Ig. Foxo3 remained in the cytosol of unstimulated and loxoribine-treated BMDCs; however, CTLA-4–Ig stimulation strongly promoted the nuclear accumulation of Foxo3 (ref. 32; **Fig. 7b**). Notably, signaling through B7 was dominant over Toll-like receptor 7 signals, as DCs treated with both loxoribine and CTLA-4–Ig showed Foxo3 nuclear localization. These experiments collectively show that CTLA-4–Ig treatment profoundly suppressed Toll-like receptor–induced production of IL-6 and TNF in wild-type DCs by promoting the nuclear accumulation of Foxo3.

If CTLA-4 signals DCs through B7-1 and B7-2, then blocking CTLA-4 should allow wild-type DCs, like Foxo3-deficient DCs, to enhance T cell survival. To investigate this issue, we cultured TCR-transgenic T cells in the presence of wild-type or *Foxo3*^{Kca} DCs and specific peptides with or without the addition of blocking antibody to CTLA-4. As expected, cultures with *Foxo3*^{Kca} BMDCs included more viable T cells than did cultures with wild-type BMDCs (**Fig. 7c**). However, the addition of anti-CTLA-4 essentially eliminated the difference in T cell accumulation and viability in these cultures. The results of these experiments are consistent with the idea that CTLA-4 is involved in promoting the nuclear localization of

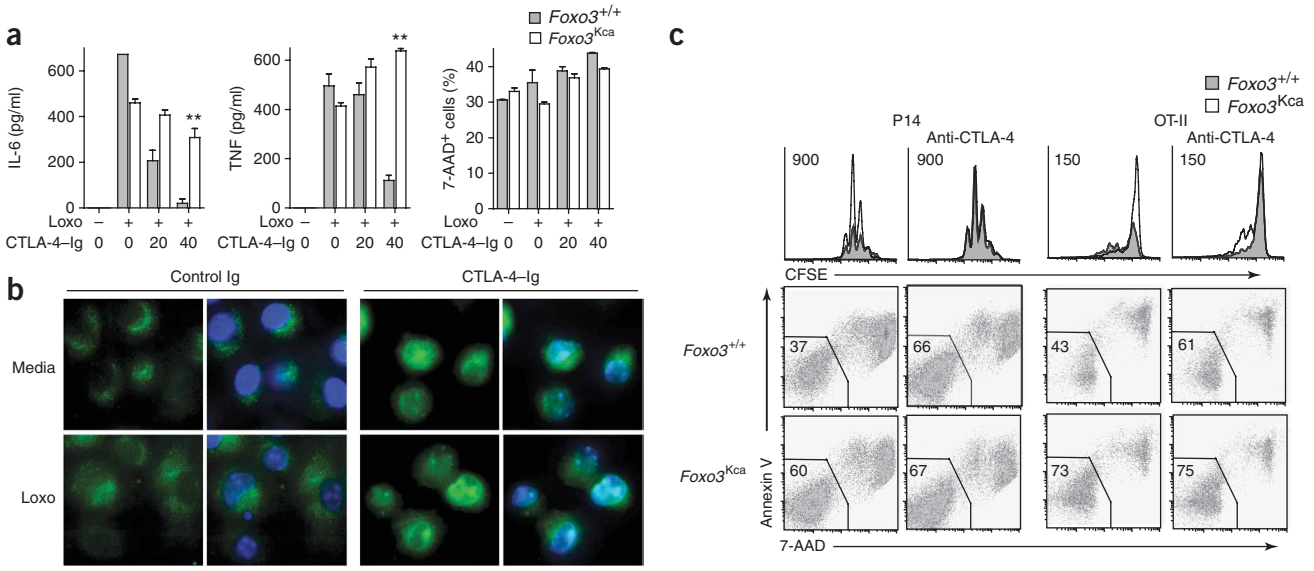

Figure 7 Production of IL-6 and TNF by stimulated DCs is inhibited by CTLA-4–Ig stimulation in a Foxo3-dependent way. (**a**) Immunoassay of the concentration of IL-6 (left) and TNF (middle) in supernatants of DCs (2×10^5) purified from the spleens of *Foxo3*^{Kca} mice and their wild-type littermates and stimulated for 18 h with (+) or without (–) loxoribine (Loxo) plus increasing amounts of CTLA-4–Ig (below graphs, in μg/ml). Right, DC viability, assessed by 7-AAD staining. (**b**) Immunofluorescence analysis of Foxo3 localization (green) after 18 h of stimulation of BMDCs from wild-type and *Foxo3*^{Kca} mice with loxoribine (bottom) or without loxoribine (Media; top) in presence of control immunoglobulin or CTLA-4–Ig. Blue, DAPI staining of nuclei. Original magnification, ×63. (**c**) Accumulation (top) and death (below) of OT-II CD4$^+$ T cells or P14 CD8$^+$ T cells (1×10^5) cultured for 3 d with wild-type or *Foxo3*^{Kca} BMDCs (3.3×10^2) in the presence of the appropriate peptide plus anti-CTLA-4 (50 μg/ml; 9D9), assessed as CFSE dilution (accumulation) and staining with annexin V and 7-AAD (death). Numbers in plots indicate number of accumulated cells (top) or percent live OT-II CD4$^+$ T cells or P14 CD8$^+$ T cells (middle and bottom). Data are representative of at least two independent experiments (error bars (**a**), s.e.m.).

Foxo3 and the resulting inhibition of inflammatory cytokines produced by DCs. Published experiments have shown that antibody specific for CTLA-4 can enhance an immune response *in vivo*[33,34], although, to our knowledge, this has not been demonstrated before in an immune response to LCMV. Nonetheless, we sought to determine whether we could detect Foxo3-dependent enhanced T cell population expansion. We inoculated mice with 100 μg of a CTLA-4-specific antibody and, 4 h later, infected the mice with LCMV. We further inoculated mice with a CTLA-4-specific antibody every other day and assessed the results on day 8. We did not find enhancement of T cell accumulation in either wild-type or Foxo3-deficient mice (**Supplementary Fig. 6** online).

DISCUSSION

In this report, we have established an essential function for Foxo3 in modulating the magnitude of antigen-specific T cell immune responses. Foxo3-deficient mice showed enhanced T cell proliferation in response to viral infection, an enhancement that was not T cell intrinsic but instead depended on the augmented capacity of DCs to sustain T cell viability. Despite the many potential targets of Foxo3, including regulators of cell cycle, apoptosis and reactive oxygen detoxification, *Foxo3* loss-of-function mutation alone had no effect on the steady-state homeostasis, survival or proliferation of T cells. That finding is consistent with studies showing that Foxo1 is essential for normal T cell homeostasis and self tolerance[16] (data not shown). Instead, we found a critical DC-intrinsic function for Foxo3 in the control of T cell responses. Foxo3 acted 'downstream' of CTLA-4-induced signals to constrain IL-6 production by DCs. The natural conditions that would override the CTLA-4-mediated nuclear localization of Foxo3 are not known; however, a new immunostimulatory cancer treatment regimen that involves blocking CTLA-4 may act in part by this mechanism[35].

Our results differ substantially from a published characterization of *Foxo3*^{Trap} mice[20]. *Foxo3*^{Trap} mutant mice were derived from an independent insertional mutant embryonic stem line obtained from BayGenomics and were backcrossed to the 129 strain for three generations. *Foxo3*^{Trap} mice show spontaneous T cell activation, lymphoproliferation and organ infiltration associated with constitutive activation of NF-κB. In contrast, we found none of those characteristics in *Foxo3*$^{-/-}$ or *Foxo3*^{Kca} mice. T cells isolated from these two strains of mice seemed to be indistinguishable from wild-type T cells in terms of NF-κB activation, expression of activation markers and response to mitogenic stimulation. Our results are consistent with published analyses of *Foxo3*^{Kca} and *Foxo3*$^{-/-}$ mice in that extensive histological analysis has not shown lymphocytic infiltration of organs[23,26].

Differences in autoimmunity are not uncommon in mixed C57BL/6 and 129 mouse strains. The 129 mice have autoimmunity-susceptibility loci, one of which (*Sle16*) induces humoral autoimmunity in congenic C57BL/6 mice. Several studies have noted modifier genes in 129 strains that confer enhanced autoimmune disease to 129 × C57BL/6 mice[36–38]. *Foxo*^{Trap} mice are apparently inbred 129 mice without a contribution from the C57BL/6 strain, but perhaps a 129 susceptibility locus that modifies the *Foxo3* deficiency is present.

IL-6 is a pleiotropic cytokine that regulates many aspects of the immune system, including antibody production, hematopoiesis, inflammation and, most relevant to our study, T cell survival[39]. IL-6 'rescues' resting T cells from apoptosis by inhibiting the downregulation of Bcl-2 in a dose-dependent way[40], and IL-6 increases the survival of antigen-stimulated T cells[31]. Consistent with that observation, we noted higher expression of Bcl-2 and Bcl-x_L in T cells from LCMV-infected *Foxo3*^{Kca} mice than in those from wild-type mice. In addition, the division rate of T cells stimulated with *Foxo3*^{Kca} DCs was not

different from that of T cells stimulated with wild-type DCs; instead, the effect was manifested as improved T cell survival. Moreover, *Foxo3*^{Kca} DCs sustained T cell viability both *in vitro* and *in vivo* even in the absence of specific peptide, which suggests that the enhanced T cell survival induced by IL-6 is not restricted to TCR-engaged T cells. Notably, IL-6-specific blocking antibody did not affect the viability of wild-type T cells *in vitro*, nor did it result in lower T cell accumulation *in vivo*. That observation indicates that in the conditions tested, the amount of IL-6 produced by wild-type DCs was not sufficient to affect T cell viability. It would be useful to determine whether immune responses to other agents are sensitive to IL-6 concentration and, in those infections, whether CTLA-4, regulatory T cells and Foxo3 affect the magnitude and dynamics of the T cell response.

CTLA-4 acts as a counterbalance to costimulation of CD28 by antagonizing TCR signals in activated T cells and by promoting tolerance[41]. CTLA-4 is also expressed on regulatory T cells and is essential for their effectiveness[42]. CTLA-4 can also modify function of cells of the immune system by triggering 'reverse signaling' through B7 receptors; these signals promote the DC production of stimulatory and/or suppressive mediators[21]. Reverse signals through B7 also activate the immunosuppressive pathway of tryptophan catabolism in plasmacytoid DCs involving indoleamine 2,3-dioxygenase (IDO)[43]. Foxo3 is involved in the IDO pathway in plasmacytoid DCs, as CTLA-4–Ig leads to nuclear accumulation of Foxo3 and expression of superoxide dismutase 2 (ref. 32). As IDO induces T cell death through the generation of kinurenin and tryptophan privation[43], we speculated that a potential IDO defect in *Foxo3*^{Kca} DCs could explain the improved T cell survival; however, addition of the IDO inhibitor 1-MT did not enhance T cell survival in cultures containing wild-type or *Foxo3*^{Kca} BMDCs (data not shown). Moreover, IDO is expressed mainly by plasmacytoid and CD8α$^+$ DC subsets[22], and low or no IDO protein is detected in resting DCs derived from bone marrow[44]. Presumably CTLA-4 expressed on regulatory T cells constitutes the main B7-stimulatory ligand, but the possibility that activated T cells or other cells contribute to B7 ligation *in vivo* has not been investigated. In addition, the relative contribution of each CTLA-4-mediated suppressive mechanism to the regulation of immune responses to various infectious agents is not well understood.

Our experiments collectively indicate that nucleus-localized Foxo3 functions in DCs to inhibit the production of inflammatory cytokines that would otherwise be activated in response to infection. We deduce that the IL-6-induced T cell survival in *Foxo3*^{Kca} mice resulted from an inability of Foxo3-deficient DCs to shut down cytokine production in response to CTLA-4 signals. Conditions that alter Foxo3 activity, such as stress, growth factors or nutrients, would be expected to substantially influence the activity of DCs and perhaps macrophages, and such conditions might be expected to alter the outcome of responses to infectious agents.

METHODS

Mice. C57BL/6, C57BL/6-CD45.1, P14, OT-I and OT-II mice were maintained in specific pathogen–free conditions at the University of California, San Diego. C57BL/6 mice lacking *Foxo3* were generated from embryonic stem cell clones from the OmniBank embryonic stem cell library of randomly targeted cell lines (Lexicon Genetics)[23]. These mice (Foxo3$^{Gt(VICTR20)1Kca}$; called '*Foxo3*^{Kca}' here) were backcrossed to the C57BL/6J strain for 12 generations and were then intercrossed to generate congenic C57BL/6 *Foxo3*^{Kca} mice. '*Foxo*$^{L/L}$' mice, with conditional targeting of *Foxo3*, were produced in FVB embryonic stem cells, and the *lox*P-flanked allele was deleted by breeding with male EIIa-Cre–transgenic mice[26]. Offspring with complete excision were bred to exclude EIIa-Cre; these mice are called '*Foxo3*$^{-/-}$' here[26]. TCR-transgenic mice with a *Foxo3*-null genotype were produced by breeding of C57BL/6 *Foxo3*^{Kca} mice with either P14 or OT-II mice. All procedures were approved by the Institutional Animal Care and Use Committee of the University of California, San Diego.

Virus infection and analysis. *Foxo3*^{Kca} mice and their wild-type littermates 6–12 weeks of age were infected by intraperitoneal injection of 2×10^5 plaque-forming units of LCMV, Armstrong strain, in 0.2 ml PBS. Alternatively, mice were infected with 1×10^5 plaque-forming units of vesicular stomatitis virus[45] expressing OVA (provided by L. Lefrançois). At various times, spleens were collected from LCMV-infected mice and uninfected control mice and splenocytes were stimulated with gp33 peptide, an MHC class I–restricted LCMV epitope (gp33-41), or gp61 peptide, an MHC class II–restricted LCMV epitope (gp61-80; Genemed Synthesis) and brefeldin A (1 μg/ml; Golgistop; BD PharMingen). After 5 h of stimulation, cells were stained for intracellular IFN-γ (XMG1.2; eBioscience). For transfer experiments, CD45.2 congenic wild-type P14 or *Foxo3*^{Kca} P14 T cells (2×10^4) were injected intravenously into CD45.1 wild-type hosts, which were infected with LCMV 24 h later. Conversely, CD45.1 congenic wild-type P14 T cells were transferred into congenic CD45.2 wild-type littermate or *Foxo3*^{Kca} mice. P14 T cells in the spleen were counted at day 8 after LCMV infection. Infection with vesicular stomatitis virus was done in an identical way except that T cells from CD45.2 OT-I mice were transferred. For bone marrow–chimera experiments, congenic CD45.1 recipient mice were lethally irradiated (1,200 rads) and were injected intravenously with 2×10^6 bone marrow cells from *Foxo3*^{Kca} or wild-type littermate donor mice (both CD45.2). After 2 months, the reconstitution of peripheral blood lymphocytes was over 90%. These radiation chimeras were then infected with LCMV and the magnitude of the LCMV response was assessed at day 8 after infection. For antibody blockade of IL-6 receptor α-chain, wild-type or Foxo3-deficient mice were inoculated intraperitoneally with 100 μg of antibody to IL-6 receptor α-chain (purified antibody to mouse and rat CD126; D7715A7; BioLegend) on day –1 and day +4 and were infected with LCMV, Armstrong strain, on day 0.

Cell isolation and purification. Bone marrow cells were isolated by flushing of the femur and tibia with RPMI medium (containing 10% (vol/vol) FBS, 2 mM L-glutamine, 100 U/ml of penicillin, 100 μg/ml of streptomycin and 50 μM β-mercaptoethanol). Spleens were removed and were incubated for 20 min at 37 °C with collagenase D (1 mg/ml; Roche), and splenocytes were collected by homogenization through a 100-μm tissue strainer. Cells were resuspended in Tris–ammonium chloride buffer for lysis of red blood cells. For purification of splenic DCs, cells were first incubated for 15 min with supernatants of 2.4G2 hybridoma cultures (anti–mouse FcγRII-III), then were incubated for 20 min with anti–mouse 'pan-DC' microbeads (Miltenyi Biotec), followed by positive selection. The positive fraction was typically over 95% CD11c$^+$. For T cell purification, splenocytes from P14 or OT-II mice were incubated with a mixture of biotinylated anti-B220 (RA3-6B2), anti-CD19, anti-Gr-1 (RB6-8C5), anti–MHC class II, anti-DX5 and anti-CD11b (M1/70; all from eBioscience) and were negatively selected to over 95% purity with strepavidin-coupled microbeads (Miltenyi Biotec).

BMDC cultures. Bone marrow cells were isolated and were cultured at a density of 2×10^6 cells/ml in RPMI medium containing recombinant mouse granulocyte-macrophage colony-stimulating factor (20 ng/ml; Peprotech). On days 2, 4 and 6, half the culture was removed and centrifuged and the cell pellet was resuspended in 10 ml fresh media containing recombinant mouse granulocyte-macrophage colony-stimulating factor (20 ng/ml). Cultures were collected on day 8 and CD11c$^+$ cells were selected with microbeads (Miltenyi Biotec). The final population was 98% CD11c$^+$CD11b$^+$B220$^-$ DCs.

Flow cytometry. Cells were incubated for 15 min with anti–mouse FcγRII-III and then were stained with primary antibodies for 20 min on ice. The following mouse monoclonal antibodies were used (all from eBioscience): allophycocyanin- or phycoerythrin-conjugated anti-CD11c (N418); fluorescein isothiocyanate– or phycoerythrin-conjugated anti-B220 (RA3-6B2); phycoerythrin-indotricarbocyanine– or peridin chlorophyll protein–conjugated anti-CD11b (M1/70); allophycocyanin-conjugated anti-CD8α (53-6.7); fluorescein isothiocyanate–conjugated anti–MHC class I and anti-Gr-1 (RB6-8C5); peridin chlorophyll protein–conjugated anti-CD3; and phycoerythrin-conjugated anti-CD86, anti-CD80, anti–MHC class II, anti-Ly6C, anti-CD19, anti-CD3 and anti-NK1.1.

T cell proliferation and death assays. For *in vitro* experiments, DCs were purified from wild-type or *Foxo3*^{Kca} mice on day 3 after LCMV infection. DCs were also purified from uninfected mice or were derived from the bone marrow of wild-type or *Foxo3*^{Kca} mice. These DCs were used to stimulated P14 CD8$^+$ T cells, OT-II CD4$^+$ T cells or OT-I CD8$^+$ T cells (1×10^5 cells per well) labeled with 1 μM CFSE (carboxyfluorescein diacetate succinimidyl ester; Molecular Probes) in the presence of gp33 peptide (0.1 μg/ml) or OVA(323–339); (1 μg/ml). Proliferation was analyzed by flow cytometry by measurement of CFSE dilution, and T cell death was measured by staining with annexin V and 7-AAD. For *in vivo* transfer experiments, CFSE-labeled CD4$^+$ T cells purified from OT-II mice were injected retro-orbitally into congenic CD45.1 C57BL/6 mice. Wild-type or *Foxo3*^{Kca} BMDCs were pulsed with OVA(323–339) and were injected intradermally after 24 h. Then, 3 d later, draining lymph nodes were collected, were stained with allophycocyanin-conjugated anti-CD4 (GK1.5) and phycoerythrin-conjugated anti-CD45.1 (A20; both from eBioscience) and were analyzed by flow cytometry.

***In vitro* stimulation of DCs and quantification of cytokine production.** Sorted DCs (2×10^5) were cultured in 96-well round-bottomed culture plates (Nunc) and were stimulated with medium alone or 0.03 mM loxoribine (InvivoGen) alone or in the presence of a recombinant mouse fusion protein consisting of the ectodomain of CTLA-4 linked to the Fc portion of IgG2a (CTLA-4–Ig) at a concentration of 20 or 40 μg/ml (R&D Systems). After culture for 18 h, supernatants were collected and cytokine concentrations were determined by immunoassay. Enzyme-linked immunosorbent assay kits were used for the detection of TNF or IL-6 (Ready-Set-Go; eBioscience) unless otherwise specified. Cytokines were also measured by cytokine bead array (BD Biosciences) or Luminex technology (Invitrogen).

Fluorescence microscopy. DCs derived from bone marrow of wild-type or *Foxo3*^{Kca} mice were cultivated for 12 h on sterile poly-L-lysine-coated coverslips (BioCoat; BD). Cells were fixed in 4% (vol/vol) formaldehyde, then were made permeable with 0.02% (vol/vol) Triton X-100. Coverslips were blocked for 2 h in PBS containing 5% (wt/vol) BSA and anti–mouse FcγRII-III. Anti-Foxo3 (FKHRL1; Cell Signaling) was added for 1 h, followed by a secondary antibody conjugated to fluorescein isothiocyanate (goat anti–rabbit IgG; 65-6111; Zymex). For staining of nuclei, DAPI (4′-6-diamidino-2-phenylindole) was added at a concentration of 0.04 μg/ml. All cells were visualized with a microscope (Axiovert 200M; Carl Zeiss MicroImaging) with a 63× objective. Images were captured with an Axiocam monochrome digital camera and were analyzed with Axiovision software (Carl Zeiss MicroImaging).

Semiquantitative RT –PCR. Total RNA was extracted from DCs with Trizol reagent according to the manufacturer's instructions (Invitrogen), then cDNA was synthesized with SuperScript First-Strand synthesis System for RT-PCR (Invitrogen). *Il6* and the gene encoding cyclophilin A (*Ppia*) were amplified by PCR with the following primers: *Il6* forward, 5′-ACCTGGAGTACATGAAGAA CAACTT-3′ and reverse, 5′-GGAAGCACTCACCTCTTGGT-3′; *Ppia* forward, 5′-CACCGTGTTCTTCGACATC-3′ and reverse, 5′-ATTCTGTGAAAGGAG GAACC-3′.

Immunoblot analysis. Equal amounts of protein from whole-cell extracts were resolved by 4–12% SDS-PAGE (Invitrogen) and were transferred to a polyvinylidene difluoride membrane (Millipore) by semidry transfer (Bio-Rad). Blots were blocked and incubated with primary antibody overnight at 4 °C, followed by 2 h of incubation at 25 °C with the appropriate horseradish peroxidase–conjugated secondary antibody. Rabbit polyclonal anti-Foxo3a was provided by A. Brunet (Stanford University). Antibodies specific for IκB proteins were from Santa Cruz Biotechnology.

Accession codes. UCSD-Nature Signaling Gateway (http://www.signaling-gateway.org): A000945 and A000706.

Note: Supplementary information is available on the Nature Immunology website.

ACKNOWLEDGMENTS

We thank J.P. Allison (Sloan-Kettering Memorial Hospital) and J.A. Bluestone (University of California at San Diego) for CTLA-4-specific blocking antibodies; A. Brunet (Stanford University) for Foxo3-specific antibody; L. Lefrançois (University of Connecticut Health Center) for OVA-expressing vesicular stomatitis virus; L. Mack and E. Zuniga for assistance with virus titers; and M. Niwa for microscope facility use. Supported by the American Cancer Society (R.A.D.), the Robert A. and Renee E. Belfer Institute for Innovative Cancer Research (R.A.D.), the US National Cancer Institute (R.A.D.), the Division of Biological Sciences of the University of California, San Diego (S.M.H.) and the Fondation pour la Recherche Médicale (A.S.D.).

AUTHOR CONTRIBUTIONS

D.R.B. initiated the project and did lymphocyte characterization and LCMV infection under the supervision of S.M.H.; A.S.D. designed and did the remaining experiments in collaboration with D.R.B., I.L.C., Y.M.K. and S.M.H.; A.B. provided expertise in fluorescence microscopy analysis; R.A.D. and D.H.C. produced *Foxo3*$^{-/-}$ mice and provided intellectual input on the data; K.C.A. provided *Foxo3*^{Kca} mice; S.M.H. initiated the project with input from R.A.D. and K.C.A. and supervised the experiments; and A.S.D. and S.M.H. wrote the manuscript with editorial and intellectual contributions from the other authors.

Published online at http://www.nature.com/natureimmunology/
Reprints and permissions information is available online at http://npg.nature.com/reprintsandpermissions/

1. Calnan, D.R. & Brunet, A. The FoxO code. *Oncogene* **27**, 2276–2288 (2008).
2. Galili, N. *et al.* Fusion of a fork head domain gene to PAX3 in the solid tumour alveolar rhabdomyosarcoma. *Nat. Genet.* **5**, 230–235 (1993).
3. Hillion, J., Le Coniat, M., Jonveaux, P., Berger, R. & Bernard, O.A. AF6q21, a novel partner of the MLL gene in t(6;11)(q21;q23), defines a forkhead transcriptional factor subfamily. *Blood* **90**, 3714–3719 (1997).
4. Corral, J. *et al.* Acute leukemias of different lineages have similar MLL gene fusions encoding related chimeric proteins resulting from chromosomal translocation. *Proc. Natl. Acad. Sci. USA* **90**, 8538–8542 (1993).
5. Jacobs, F.M. *et al.* FoxO6, a novel member of the FoxO class of transcription factors with distinct shuttling dynamics. *J. Biol. Chem.* **278**, 35959–35967 (2003).
6. Barthel, A., Schmoll, D. & Unterman, T.G. FoxO proteins in insulin action and metabolism. *Trends Endocrinol. Metab.* **16**, 183–189 (2005).
7. Biggs, W.H. III, Meisenhelder, J., Hunter, T., Cavenee, W.K. & Arden, K. C. Protein kinase B/Akt-mediated phosphorylation promotes nuclear exclusion of the winged helix transcription factor FKHR1. *Proc. Natl. Acad. Sci. USA* **96**, 7421–7426 (1999).
8. Brunet, A. *et al.* Akt promotes cell survival by phosphorylating and inhibiting a Forkhead transcription factor. *Cell* **96**, 857–868 (1999).
9. Kops, G.J. *et al.* Direct control of the Forkhead transcription factor AFX by protein kinase B. *Nature* **398**, 630–634 (1999).
10. van der Horst, A. & Burgering, B.M. Stressing the role of FoxO proteins in lifespan and disease. *Nat. Rev. Mol. Cell Biol.* **8**, 440–450 (2007).
11. Brunet, A. *et al.* Stress-dependent regulation of FOXO transcription factors by the SIRT1 deacetylase. *Science* **303**, 2011–2015 (2004).
12. Motta, M.C. *et al.* Mammalian SIRT1 represses forkhead transcription factors. *Cell* **116**, 551–563 (2004).
13. Stahl, M. *et al.* The forkhead transcription factor FoxO regulates transcription of p27Kip1 and Bim in response to IL-2. *J. Immunol.* **168**, 5024–5031 (2002).
14. Dijkers, P.F. *et al.* Forkhead transcription factor FKHR-L1 modulates cytokine-dependent transcriptional regulation of p27^{KIP1}. *Mol. Cell. Biol.* **20**, 9138–9148 (2000).
15. Barata, J.T. *et al.* Activation of PI3K is indispensable for interleukin 7-mediated viability, proliferation, glucose use, and growth of T cell acute lymphoblastic leukemia cells. *J. Exp. Med.* **200**, 659–669 (2004).
16. Kerdiles, Y.M. *et al.* Foxo1 links homing and survival of naive T cells by regulating L-selectin, CCR7 and interleukin 7 receptor. *Nat. Immunol.* **10**, 176–184 (2009).
17. Peng, S.L. Foxo in the immune system. *Oncogene* **27**, 2337–2344 (2008).
18. You, H. *et al.* FOXO3a-dependent regulation of Puma in response to cytokine/growth factor withdrawal. *J. Exp. Med.* **203**, 1657–1663 (2006).
19. Riou, C. *et al.* Convergence of TCR and cytokine signaling leads to FOXO3a phosphorylation and drives the survival of CD4$^+$ central memory T cells. *J. Exp. Med.* **204**, 79–91 (2007).
20. Lin, L., Hron, J.D. & Peng, S.L. Regulation of NF-κB, Th activation, and autoinflammation by the forkhead transcription factor Foxo3a. *Immunity* **21**, 203–213 (2004).
21. Orabona, C. *et al.* CD28 induces immunostimulatory signals in dendritic cells via CD80 and CD86. *Nat. Immunol.* **5**, 1134–1142 (2004).
22. Mellor, A.L. & Munn, D.H. IDO expression by dendritic cells: tolerance and tryptophan catabolism. *Nat. Rev. Immunol.* **4**, 762–774 (2004).
23. Hosaka, T. *et al.* Disruption of forkhead transcription factor (FOXO) family members in mice reveals their functional diversification. *Proc. Natl. Acad. Sci. USA* **101**, 2975–2980 (2004).
24. Marinkovic, D. *et al.* Foxo3 is required for the regulation of oxidative stress in erythropoiesis. *J. Clin. Invest.* **117**, 2133–2144 (2007).
25. Greer, E.L. & Brunet, A. FOXO transcription factors at the interface between longevity and tumor suppression. *Oncogene* **24**, 7410–7425 (2005).
26. Castrillon, D.H., Miao, L., Kollipara, R., Horner, J.W. & DePinho, R.A. Suppression of ovarian follicle activation in mice by the transcription factor Foxo3a. *Science* **301**, 215–218 (2003).

27. Villadangos, J.A. & Schnorrer, P. Intrinsic and cooperative antigen-presenting functions of dendritic-cell subsets *in vivo*. *Nat. Rev. Immunol.* **7**, 543–555 (2007).
28. Oldstone, M.B. Biology and pathogenesis of lymphocytic choriomeningitis virus infection. *Curr. Top. Microbiol. Immunol.* **263**, 83–117 (2002).
29. Rosas, M. *et al.* IL-5-mediated eosinophil survival requires inhibition of GSK-3 and correlates with β-catenin relocalization. *J. Leukoc. Biol.* **80**, 186–195 (2006).
30. Korn, T., Bettelli, E., Oukka, M. & Kuchroo, V.K. IL-17 and Th17 cells. *Annu. Rev. Immunol.* **27**, 485–517 (2009).
31. Rochman, I., Paul, W.E. & Ben-Sasson, S.Z. IL-6 increases primed cell expansion and survival. *J. Immunol.* **174**, 4761–4767 (2005).
32. Fallarino, F. *et al.* CTLA-4-Ig activates forkhead transcription factors and protects dendritic cells from oxidative stress in nonobese diabetic mice. *J. Exp. Med.* **200**, 1051–1062 (2004).
33. Leach, D.R., Krummel, M.F. & Allison, J.P. Enhancement of antitumor immunity by CTLA-4 blockade. *Science* **271**, 1734–1736 (1996).
34. Karandikar, N.J., Vanderlugt, C.L., Walunas, T.L., Miller, S.D. & Bluestone, J.A. CTLA-4: a negative regulator of autoimmune disease. *J. Exp. Med.* **184**, 783–788 (1996).
35. Zang, X. & Allison, J.P. The B7 family and cancer therapy: costimulation and coinhibition. *Clin. Cancer Res.* **13**, 5271–5279 (2007).
36. Botto, M. *et al.* Homozygous C1q deficiency causes glomerulonephritis associated with multiple apoptotic bodies. *Nat. Genet.* **19**, 56–59 (1998).
37. Bickerstaff, M.C. *et al.* Serum amyloid P component controls chromatin degradation and prevents antinuclear autoimmunity. *Nat. Med.* **5**, 694–697 (1999).
38. Santiago-Raber, M.L. *et al.* Role of cyclin kinase inhibitor p21 in systemic autoimmunity. *J. Immunol.* **167**, 4067–4074 (2001).
39. Kishimoto, T. Interleukin-6: from basic science to medicine–40 years in immunology. *Annu. Rev. Immunol.* **23**, 1–21 (2005).
40. Teague, T.K., Marrack, P., Kappler, J.W. & Vella, A.T. IL-6 rescues resting mouse T cells from apoptosis. *J. Immunol.* **158**, 5791–5796 (1997).
41. Keir, M.E. & Sharpe, A.H. The B7/CD28 costimulatory family in autoimmunity. *Immunol. Rev.* **204**, 128–143 (2005).
42. Wing, K. *et al.* CTLA-4 control over Foxp3$^+$ regulatory T cell function. *Science* **322**, 271–275 (2008).
43. Grohmann, U. *et al.* CTLA-4-Ig regulates tryptophan catabolism *in vivo*. *Nat. Immunol.* **3**, 1097–1101 (2002).
44. Hara, T. *et al.* High-affinity uptake of kynurenine and nitric oxide-mediated inhibition of indoleamine 2,3-dioxygenase in bone marrow-derived myeloid dendritic cells. *Immunol. Lett.* **116**, 95–102 (2008).
45. van Stipdonk, M.J., Lemmens, E.E. & Schoenberger, S.P. Naive CTLs require a single brief period of antigenic stimulation for clonal expansion and differentiation. *Nat. Immunol.* **2**, 423–429 (2001).